Monthly Notices
of the
ROYAL ASTRONOMICAL SOCIETY

MNRAS **433,** 1262–1270 (2013)
Advance Access publication 2013 May 30

doi:10.1093/mnras/stt802

Interferometric radii of bright *Kepler* stars with the CHARA Array: θ Cygni and 16 Cygni A and B

T. R. White,[1,2,3]★ D. Huber,[1,4]† V. Maestro,[1] T. R. Bedding,[1,3] M. J. Ireland,[1,2,5] F. Baron,[6] T. S. Boyajian,[7,8] X. Che,[6] J. D. Monnier,[6] B. J. S. Pope,[1] R. M. Roettenbacher,[6] D. Stello,[1,3] P. G. Tuthill,[1] C. D. Farrington,[7] P. J. Goldfinger,[7] H. A. McAlister,[7] G. H. Schaefer,[7] J. Sturmann,[7] L. Sturmann,[7] T. A. ten Brummelaar[7] and N. H. Turner[7]

[1]*Sydney Institute for Astronomy (SIfA), School of Physics, University of Sydney, NSW 2006, Australia*
[2]*Australian Astronomical Observatory, PO Box 296, Epping, NSW 1710, Australia*
[3]*Stellar Astrophysics Centre, Department of Physics and Astronomy, Aarhus University, Ny Munkegade 120, DK-8000 Aarhus C, Denmark*
[4]*NASA Ames Research Center, MS 244-30, Moffett Field, CA 94035, USA*
[5]*Department of Physics and Astronomy, Macquarie University, NSW 2109, Australia*
[6]*Department of Astronomy, University of Michigan, 941 Dennison Bldg, Ann Arbor, MI 48109-1090, USA*
[7]*Center for High Angular Resolution Astronomy, Georgia State University, PO Box 3969, Atlanta, GA 30302, USA*
[8]*Department of Astronomy, Yale University, 260 Whitney Ave, New Haven, CT 06520, USA*

Accepted 2013 May 7. Received 2013 May 3; in original form 2013 March 31

ABSTRACT

We present the results of long-baseline optical interferometry observations using the Precision Astronomical Visual Observations (PAVO) beam combiner at the Center for High Angular Resolution Astronomy (CHARA) Array to measure the angular sizes of three bright *Kepler* stars: θ Cygni, and both components of the binary system 16 Cygni. Supporting infrared observations were made with the Michigan Infrared Combiner (MIRC) and Classic beam combiner, also at the CHARA Array. We find limb-darkened angular diameters of 0.753 ± 0.009 mas for θ Cyg, 0.539 ± 0.007 mas for 16 Cyg A and 0.490 ± 0.006 mas for 16 Cyg B. The *Kepler Mission* has observed these stars with outstanding photometric precision, revealing the presence of solar-like oscillations. Due to the brightness of these stars the oscillations have exceptional signal-to-noise, allowing for detailed study through asteroseismology, and are well constrained by other observations. We have combined our interferometric diameters with Hipparcos parallaxes, spectrophotometric bolometric fluxes and the asteroseismic large frequency separation to measure linear radii (θ Cyg: 1.48 ± 0.02 $R_\odot$, 16 Cyg A: 1.22 ± 0.02 $R_\odot$, 16 Cyg B: 1.12 ± 0.02 $R_\odot$), effective temperatures (θ Cyg: 6749 ± 44 K, 16 Cyg A: 5839 ± 42 K, 16 Cyg B: 5809 ± 39 K) and masses (θ Cyg: 1.37 ± 0.04 $M_\odot$, 16 Cyg A: 1.07 ± 0.05 $M_\odot$, 16 Cyg B: 1.05 ± 0.04 $M_\odot$) for each star with very little model dependence. The measurements presented here will provide strong constraints for future stellar modelling efforts.

Key words: techniques: interferometric – stars: individual: θ Cygni – stars: individual: 16 Cygni A – stars: individual: 16 Cygni B – stars: oscillations.

1 INTRODUCTION

Progress in understanding stellar structure and evolution is driven by ever-more precise measurements of fundamental properties such as stellar temperature, radius and mass (see e.g. Demarque, Guenther & van Altena 1986; Monteiro, Christensen-Dalsgaard & Thompson 1996; Deheuvels & Michel 2011; Piau et al. 2011; Trampedach & Stein 2011). Unfortunately, many methods to determine such properties are indirect and, being model dependent themselves, are of little use in improving stellar models. We therefore look towards methods that either themselves, or in combination with other methods, have little model dependence.

One such method is asteroseismology, the study of stellar oscillations. Stars like the Sun exhibit many convectively excited

★ E-mail: t.white@physics.usyd.edu.au
† NASA Postdoctoral Program Fellow.

oscillation modes whose properties depend on the structure of the star. This allows stellar parameters such as mean stellar density and surface gravity to be accurately determined with little model dependence (see e.g. Brown & Gilliland 1994; Christensen-Dalsgaard 2004; Aerts, Christensen-Dalsgaard & Kurtz 2010).

Another method is long-baseline optical interferometry (LBOI), which can be used to measure the angular sizes of stars. Combining with a parallax measurement yields the linear radius, while combining with the bolometric flux provides a direct measurement of effective temperature (see e.g. Code et al. 1976; Baines et al. 2009; Boyajian et al. 2009, 2012a,b; Creevey et al. 2012).

The combination of asteroseismology and interferometry therefore allows us to determine mass, radius and temperature with very little model dependence. While the potential value of this has long been recognized (Cunha et al. 2007), until recently the inherent difficulties in these methods had limited their application in cool stars to a few bright objects (North et al. 2007; Bruntt et al. 2010; Bazot et al. 2011). Progress in instrumentation, such as the Precision Astronomical Visible Observations (PAVO) beam combiner (Ireland et al. 2008) at the Center for High Angular Resolution Astronomy (CHARA) Array (ten Brummelaar et al. 2005), has pushed the sensitivity limits of LBOI. Meanwhile asteroseismology has entered a 'golden age', thanks to data from the space telescopes *CoRoT* (Michel et al. 2008) and *Kepler* (Gilliland et al. 2010; Koch et al. 2010; Chaplin et al. 2011).

Huber et al. (2012b) recently presented interferometric observations using the PAVO beam combiner at CHARA of F, G and K stars spanning from the main sequence to the red clump in which solar-like oscillations have been detected by *Kepler* or *CoRoT*. In this paper, we present results from the same instrument, of three bright *Kepler* targets, θ Cygni and 16 Cygni A and B. These targets present an excellent opportunity to combine the remarkably precise, high signal-to-noise asteroseismology data from the *Kepler Mission* with precise constraints from interferometry and other methods for strong tests of stellar models.

2 TARGETS

2.1 θ Cyg

The F4V star θ Cygni (13 Cyg, HR 7469, HD 185395, KIC 11918630), magnitude $V = 4.48$, is the brightest star being observed by *Kepler*. Stellar parameters available from the literature are given in Table 1. Thus far, *Kepler* has observed it in 2010 June–September (*Kepler* Quarter 6), 2011 January–March (Q8) and 2012 January–October (Q12–Q14).

A close companion of $V \sim 12$ mag has been identified as an M dwarf, with an estimated mass of 0.35 $M_\odot$, separated from the primary by ∼2 arcsec, a projected separation of 46 au (Desort et al. 2009). Although it has been detected several times since 1889 (Mason et al. 2001), the orbit is still very incomplete.

Desort et al. (2009) undertook a radial velocity study of θ Cyg, finding a 150 d quasi-periodic variation. The origin of this variation is still not satisfactorily explained – the presence of one or two planets does not adequately explain all the observations and stellar variation of this period is unknown in stars of this type.

The limb-darkened angular diameter of θ Cyg has previously been estimated as $\theta_{LD} = 0.760 \pm 0.021$ mas from spectral energy distribution fitting to photometric observations by van Belle et al. (2008). In 2007 and 2008, Boyajian et al. (2012a) made interferometric observations with the CHARA Classic beam combiner in K' band ($\lambda_0 = 2.14\,\mu$m). They measured a larger diameter, $\theta_{LD} =$ 0.861 ± 0.015 mas. Ligi et al. (2012), using the Visible spEctroGraph and polArimeter (VEGA) beam combiner at CHARA found $\theta_{LD} = 0.760 \pm 0.003$ mas, in agreement with van Belle et al. (2008). Ligi et al. (2012) also reported excessive scatter in their measurements and speculated on diameter variability or the existence of a new close companion, possibly related to the quasi-periodic variability seen in radial velocity by Desort et al. (2009).

The location of θ Cyg in the Hertzsprung–Russell (HR) diagram places it amongst γ Dor pulsators. Analysis of Q6 *Kepler* data by Guzik et al. (2011) did not reveal γ Dor pulsations, but clear evidence of solar-like oscillations was seen in the power spectrum between 1200 and 2500 μHz. The characteristic large frequency separation between modes of the same spherical degree, $\Delta\nu$, is 84.0 ± 0.2 μHz. The oscillation modes are significantly damped resulting in large linewidths in the power spectrum, which is typical of F stars (Chaplin et al. 2009; Baudin et al. 2011; Appourchaux et al. 2012; Corsaro et al. 2012).

Table 1. Properties of target stars from available literature.

	θ Cyg	16 Cyg A	16 Cyg B
Spectral type	F4V	G1.5V	G3V
V mag	4.48	5.96	6.2
$T_{\rm eff}$ (K)	6745 ± 150^a	5825 ± 50^b	5750 ± 50^b
log g	4.2 ± 0.2^a	4.33 ± 0.07^b	4.34 ± 0.07^b
[Fe/H]	-0.03^a	0.096 ± 0.026^b	0.052 ± 0.021^b
Parallax (mas)	54.54 ± 0.15^c	47.44 ± 0.27^c	47.14 ± 0.27^c
Distance (pc)	18.33 ± 0.05	21.08 ± 0.12	21.21 ± 0.12
$F_{\rm bol}$ (pW . m^{-2})	392.0 ± 0.4^d	112.5 ± 0.2^d	91.08 ± 0.14^d
Luminosity ($L_\odot$)	4.11 ± 0.02	1.56 ± 0.02	1.28 ± 0.01
Mass ($M_\odot$)	$1.39^{+0.02}_{-0.01}{}^e$	1.11 ± 0.02^f	1.07 ± 0.02^f
Radius ($R_\odot$)	–	1.243 ± 0.008^f	1.127 ± 0.007^f
Age (Gyr)	$1.13^{+0.17}_{-0.21}{}^e$	6.9 ± 0.3^f	6.7 ± 0.4^f

[a]Erspamer & North (2003), high-resolution spectroscopy.
[b]Ramírez, Meléndez & Asplund (2009), high-resolution spectroscopy.
[c]van Leeuwen (2007), revised Hipparcos parallax.
[d]Boyajian et al. (2013), spectrophotometry.
[e]Casagrande et al. (2011), fit to isochrones.
[f]Metcalfe et al. (2012), asteroseismology.

2.2 16 Cyg A and B

Our other targets are the solar analogues 16 Cygni A (HR 7503, HD 186408, KIC 12069424) and B (HR 7504, HD 186427, KIC 12069449). Properties of the stars from the literature are listed in Table 1. *Kepler* observations between 2010 June and 2012 October (Q6–Q14) are currently available.

The separation of the A and B components on the sky is 39.56 arcsec, which enables them to be observed independently by both *Kepler* and PAVO. They also have a distant M dwarf companion, about 10 mag fainter, in a hierarchical triple system (Turner et al. 2001; Patience et al. 2002). There are, however, no dynamical constraints on their masses due to the long orbital period, estimated at over 18 000 yr (Hauser & Marcy 1999). Additionally, 16 Cyg B is known to have a planet with a mass of ∼1.5 M_J in an eccentric 800 d orbit (Cochran et al. 1997).

Interferometric observations of 16 Cyg A and B with the CHARA Classic beam combiner have been presented previously. Observing in K' band, Baines et al. (2008) measured a limb-darkened angular diameter for 16 Cyg B of $\theta_{LD} = 0.426 \pm 0.056$ mas, although their estimate from a spectral energy distribution fit was somewhat larger ($\theta_{LD} = 0.494 \pm 0.019$ mas). More recently, Boyajian et al.

(2013) measured both stars with Classic in H band ($\lambda_0 = 1.65$ μm), finding $\theta_{\rm LD} = 0.554 \pm 0.011$ and 0.513 ± 0.012 mas for the A and B components, respectively.

Kepler observations clearly show solar-like oscillations in both stars, with large separations, $\Delta\nu$, of 103.4 and 117.0 μHz, respectively (Metcalfe et al. 2012). Asteroseismic modelling was performed by Metcalfe et al. (2012) using several different methods. The values they obtained for mass, radius and age are given in Table 1. Promisingly, although both stars were modelled independently, the models find a common age and initial composition, which is to be expected in a binary system. However, inspecting the individual results of each model method reveals two families of solutions. Several models favour a radius of $1.24\,R_\odot$ for 16 Cyg A and $1.12\,R_\odot$ for 16 Cyg B, while others favour a larger radii around 1.26 and $1.14\,R_\odot$, respectively. For comparison, the estimated systematic uncertainties in radius are 0.008 and $0.007\,R_\odot$, respectively.

3 OBSERVATIONS

Our interferometric observations were made with the PAVO beam combiner (Ireland et al. 2008) at the CHARA Array at Mt. Wilson Observatory, California (ten Brummelaar et al. 2005). PAVO is a pupil-plane beam combiner, optimized for high sensitivity (limiting magnitude in typical seeing conditions of $R \sim 8$) at visible wavelengths (∼600–900 nm). Two or three beams may be combined. Through spectral dispersion each scan typically produces visibility measurements in 20 independent wavelength channels. With available baselines up to 330 m, PAVO at CHARA is one of the highest angular-resolution instruments operating worldwide. Further details on this instrument were given by Ireland et al. (2008). Early PAVO science results have been presented by Bazot et al. (2011), Derekas et al. (2011), Huber et al. (2012a,b) and Maestro et al. (2012).

Most of our observations were made during several nights in 2012 August, although some data were taken during previous observing seasons in 2010 and 2011. Our observations have been made using PAVO in two-telescope mode, with baselines ranging from 110 to 250 m. A summary of our observations is given in Table 2. To calibrate the fringe visibilities in our targets, we observed nearby stars, which ideally would be unresolved point sources with no close companions. In practice, we used stars as unresolved as possible, which in our case meant spectral types A and B. Table 3 lists the calibrators used in our analysis. We determined the expected angular diameters of the calibrators using the $(V - K)$ relation of Kervella et al. (2004). We adopted V-band magnitudes from the Tycho catalogue (Perryman & ESA 1997) and converted them into the Johnson system using the calibration by Bessell (2000). K-band magnitudes were taken from the Two Micron All Sky Survey (Skrutskie et al. 2006). To de-redden the photometry, we used the extinction model of Drimmel, Cabrera-Lavers & López-Corredoira (2003) to estimate interstellar reddening, and adopted the reddening law of O'Donnell (1994) (see also Cardelli, Clayton & Mathis 1989).

In the case of our largest calibrator, HD 188665, there is some indication that it is larger than expected from the $(V - K)$ relation ($\theta_{V-K} = 0.240$ mas). Calibrating with smaller calibrator stars observed at similar times we find the average interferometric response of HD 188665 is consistent with a uniform-disc diameter of $\theta_{UD} = 0.274 \pm 0.008$ mas.

To best account for temporal variations in system visibility due to changes in seeing, calibrators must be observed as closely spaced in time to the targets as possible. We observed θ Cyg and its calibrators in the sequence: *calibrator 1 – θ Cyg – calibrator 2*, with a scan of each object obtaining 2 minutes of visibility data. Such a sequence typically lasted 15 minutes, including slewing. To minimize slew times when observing 16 Cyg A and B, we observed in the sequence: *calibrator 1 – 16 Cyg A – 16 Cyg B – calibrator 2*. This typically took 20 minutes.

In addition to our observations with PAVO, supporting observations were also made in the infrared with two other beam combiners at the CHARA Array. Observations of θ Cyg were made using the Michigan Infrared Combiner (MIRC; Monnier et al. 2004), while observations of 16 Cyg A and B were made with the CHARA Classic combiner.

MIRC combines up to six telescope beams in the image plane, allowing for simultaneous visibility measurements on 15 baselines and 20 closure phase measurements. Additionally, MIRC

Table 2. Log of PAVO interferometric observations.

UT date	Baseline[a]	Target	No. of scans	Calibrators[b]
2010 July 20	S2E2	16 Cyg A	1	c
2011 May 27	E2W2	θ Cyg	3	ij
2011 May 28	E2W2	θ Cyg	2	b
2011 July 4	S1W2	16 Cyg A	3	bh
		16 Cyg B	3	bh
2011 September 9	S2W2	16 Cyg A	3	be
		16 Cyg B	3	be
2012 August 4	S1W2	16 Cyg A	3	aeg
		16 Cyg B	3	aeg
		θ Cyg	3	aegi
2012 August 6	E2W2	θ Cyg	4	egi
2012 August 8	S1W2	16 Cyg A	3	afi
		16 Cyg B	3	afi
		θ Cyg	3	afgi
2012 August 9	S2E2	16 Cyg A	3	fgi
		16 Cyg B	3	fgi
2012 August 10	S2W2	16 Cyg A	2	bdi
		16 Cyg B	2	dfi
		θ Cyg	3	fgi
2012 August 11	W1W2	θ Cyg	1	i
2012 August 12	E2W1	16 Cyg A	3	fik
		16 Cyg B	3	fik
2012 August 14	S2E2	16 Cyg A	3	fgi
		16 Cyg B	3	fgi

[a]The baselines used have the following lengths:
W1W2, 107.92 m; E2W2, 156.27 m; S2W2, 177.45 m; S1W2, 210.97 m; S2E2, 248.13 m; E2W1, 251.34 m.
[b]Refer to Table 3 for details of the calibrators used.

Table 3. Calibrators used for interferometric observations.

HD	Sp. type	V	$V - K$	$E(B - V)$	θ_{V-K}	ID
176626	A2V	6.85	0.084	0.026	0.146	a
177003	B2.5IV	5.38	− 0.524	0.023	0.198	b
179483	A2V	7.21	0.316	0.028	0.144	c
180681	A0V	7.50	0.112	0.031	0.111	d
181960	A1V	6.23	0.121	0.042	0.200	e
183142	B8V	7.07	− 0.462	0.060	0.093	f
184787	A0V	6.68	0.034	0.017	0.154	g
188252	B2III	5.90	− 0.461	0.047	0.156	h
188665[a]	B5V	5.14	− 0.384	0.035	0.240	i
189296	A4V	6.16	0.250	0.033	0.225	j
190025	B5V	7.55	− 0.230	0.157	0.084	k

[a]For this star we instead use the calibrated diameter, $\theta_{\rm UD} = 0.274 \pm 0.008$ (see the text).

Table 4. Measured angular diameters and fundamental properties.

Star	Combiner	μ	$\theta_{\rm UD}$ (mas)	$\theta_{\rm LD}$ (mas)	R ($R_\odot$)	M ($M_\odot$)	$T_{\rm eff}$ (K)
θ Cyg	PAVO	0.47 ± 0.04	0.720 ± 0.004	0.754 ± 0.009	1.49 ± 0.02	1.37 ± 0.04	6745 ± 44
	MIRC	0.21 ± 0.03	0.726 ± 0.014	0.739 ± 0.015	1.46 ± 0.03	1.31 ± 0.06	6813 ± 72
	PAVO+MIRC	–	–	0.753 ± 0.009	1.48 ± 0.02	1.37 ± 0.04	6749 ± 44
16 Cyg A	PAVO	0.54 ± 0.04	0.513 ± 0.004	0.539 ± 0.006	1.22 ± 0.02	1.07 ± 0.04	5839 ± 37
	Classic	0.26 ± 0.04	0.542 ± 0.015	0.554 ± 0.016	1.26 ± 0.04	1.16 ± 0.10	5759 ± 85
	PAVO+Classic	–	–	0.539 ± 0.007	1.22 ± 0.02	1.07 ± 0.05	5839 ± 42
16 Cyg B	PAVO	0.56 ± 0.04	0.467 ± 0.004	0.490 ± 0.006	1.12 ± 0.02	1.05 ± 0.04	5809 ± 39
	Classic	0.27 ± 0.04	0.502 ± 0.020	0.513 ± 0.020	1.17 ± 0.05	1.20 ± 0.14	5680 ± 112
	PAVO+Classic	–	–	0.490 ± 0.006	1.12 ± 0.02	1.05 ± 0.04	5809 ± 39

splits the H-band light ($\lambda_0 = 1.65\,\mu$m) into eight independent spectral channels. Further details on the MIRC instrument may be found in Monnier et al. (2004, 2006, 2010), Che, Monnier & Webster (2010) and Che et al. (2012). Our MIRC observations consist of four scans of θ Cyg, made in six-telescope mode on 2012 June 19. The calibrator star used was σ Cyg, with an assumed diameter of $\theta_{UD} = 0.54 \pm 0.02$ mas (Barnes, Evans & Moffett 1978).

Classic is a pupil-plane combiner operating in a two-telescope mode in either of H band ($\lambda_0 = 1.65\,\mu$m) or K' band ($\lambda_0 = 2.14\,\mu$m). The Classic observations of 16 Cyg A and B were previously presented by Boyajian et al. (2013). Observations were made in H band, with 23 and 24 brackets of 16 Cyg A and B, respectively, over the nights of 2012 August 16, 19, 20 and 21 using the S1E1, E1W1 and S1W1 baselines. Calibration stars were HD 185414, HD 191096 and HD 191195, whose estimated angular diameters were taken from the SearchCal tool developed by the JMMC Working Group (Bonneau et al. 2006, 2011).

For each target, we fitted a limb-darkened disc model to the visibility measurements (Hanbury Brown et al. 1974),

$$V = \left(\frac{1-\mu_\lambda}{2} + \frac{\mu_\lambda}{3}\right)^{-1} \times \left[(1-\mu_\lambda)\frac{J_1(x)}{x} + \mu_\lambda(\pi/2)^{1/2}\frac{J_{3/2}(x)}{x^{3/2}}\right], \quad (1)$$

where

$$x = \pi B \theta_{\rm LD} \lambda^{-1}. \quad (2)$$

Here, V is the visibility, μ_λ is the linear limb-darkening coefficient, $J_n(x)$ is the nth-order Bessel function, B is the projected baseline, $\theta_{\rm LD}$ is the angular diameter after correction for limb darkening and λ is the wavelength at which the observations was made. The quantity $B\lambda^{-1}$ is often referred to as the spatial frequency.

We determined linear limb-darkening coefficients in the R and H bands for our targets by interpolating the model grid by Claret & Bloemen (2011) to the spectroscopic estimates of $T_{\rm eff}$, log g and [Fe/H] given in Table 1 for a microturbulent velocity of 2 km s^{-1}. The uncertainties in the spectroscopic parameters were used to create 1000 realizations of the limb-darkening coefficients, from which the uncertainties were estimated. Adopted values of the linear limb-darkening coefficients are given in Table 4. Typically, the influence of the adopted limb darkening on the final fitted angular diameter is relatively small. Detailed 3D hydrodynamical models by Bigot et al. (2006), Chiavassa et al. (2010) and Chiavassa et al. (2012) for dwarfs and giants have shown that the differences from simple linear limb-darkening models are ∼1 per cent or less in angular diameter for stars with near-solar metallicity. For a moderately well-resolved star with $V^2 \sim 0.5$, a 1 per cent change in angular diameter would correspond to an uncertainty of less than 1 per cent in V^2. For our measurements these effects may be non-negligible and our results will be valuable for comparing simple 1D to sophisticated 3D models.

To fit the model and estimate the uncertainty in the derived angular diameters, we followed the procedure outlined by Derekas et al. (2011). This involved performing Monte Carlo simulations, taking into account uncertainties in the data, adopted wavelength calibration (0.5 per cent for PAVO, 0.25 per cent for MIRC), calibrator sizes (5 per cent) and limb-darkening coefficients (see Table 4).

4 RESULTS

4.1 Fundamental stellar properties

Combining our interferometric measurements with astrometric, asteroseismic and photometric measurements allows us to derive radii, masses and effective temperatures that are nearly model independent.

The linear radius, R, is

$$R = \frac{1}{2}\theta_{\rm LD} D, \quad (3)$$

where D is the distance to the star, which itself is obtained directly from the parallax.

From an estimate of the bolometric flux at Earth, $F_{\rm bol}$, we can find the effective temperature,

$$T_{\rm eff} = \left(\frac{4F_{\rm bol}}{\sigma\theta_{\rm LD}^2}\right)^{1/4}, \quad (4)$$

where σ is the Stefan–Boltzmann constant.

Finally, to obtain the mass we use the scaling relation between the large frequency separation of solar-like oscillations, $\Delta\nu$, and the density of the star (Ulrich 1986):

$$\frac{\Delta\nu}{\Delta\nu_\odot} = \left(\frac{M}{M_\odot}\right)^{1/2}\left(\frac{R}{R_\odot}\right)^{-3/2}. \quad (5)$$

It follows from this relation that we can derive the mass of the star from measurements of the angular diameter, parallax and large frequency separation. Caution is required when using this relationship because the assumption that leads to this relation, that other stars are homologous to the Sun, is not strictly valid (Belkacem 2012), although it has been shown that the relation holds to within 5 per cent in models (Stello et al. 2009a; White et al. 2011). Particular care is needed for stars above 1.2 $M_\odot$ and beyond the main sequence, since models indicate a departure that is largely a function of effective temperature (White et al. 2011). We note that one should measure $\Delta\nu$ of the stars and the Sun in a self-consistent manner. We adopt a solar value of $\Delta\nu_\odot = 135.1\,\mu$Hz.

4.2 θ Cyg

Fig. 1 presents the calibrated squared-visibility measurements as a function of spatial frequency for θ Cyg. We have performed limb-darkened fits to the PAVO and MIRC data both separately and together. For the combined fit, we fitted a common angular diameter, but applied a different linear limb-darkening coefficient to the MIRC and PAVO data. Provided the star has a compact atmosphere, the limb-darkened angular diameter should be independent of wavelength. We also fitted uniform-disc models separately. Uniform-disc diameters are wavelength dependent due to the effects of limb darkening.

The fitted angular diameters are given in Table 4, along with the radius, mass and effective temperature (see Section 4.1). We note that our diameter ($\theta_{\rm LD} = 0.753 \pm 0.009$ mas) is consistent with that obtained recently by Ligi et al. (2012, $\theta_{\rm LD} = 0.760 \pm 0.003$ mas), as well as the estimation by van Belle et al. (2008, $\theta_{\rm LD} = 0.760 \pm 0.021$ mas). The values found by Boyajian et al. (2012a, $\theta_{\rm UD} = 0.845 \pm 0.015$ and $\theta_{\rm LD} = 0.861 \pm 0.015$ mas) are inconsistent with our data. Operating at higher spatial frequencies, PAVO is better able to resolve θ Cyg than Classic. With the lower resolution of Classic, calibration errors have greater impact and this could explain the discrepancy.

We note that the uncertainty in the PAVO diameter is dominated by our adopted uncertainties in the limb-darkening coefficient rather than measurement uncertainties. Uncertainties in the calibrator sizes and wavelength scale also make significant contributions to the overall error budget. For comparison, ignoring these uncertainties in fitting the PAVO data yields a fractional uncertainty of only 0.2 per cent compared to an uncertainty of 1.2 per cent derived from our Monte Carlo simulations. This illustrates the importance of taking into account these additional uncertainties.

To determine the mass, we have used the revised scaling relation for $\Delta\nu$ proposed by White et al. (2011), which corrects for a deviation from the original scaling relation that is dependent upon effective temperature. Without this correction we obtain a significantly lower mass for θ Cyg (1.27 $M_\odot$) that is not consistent with the value of $1.39^{+0.02}_{-0.01}$ $M_\odot$ obtained from isochrones by Casagrande et al. (2011) in their re-analysis of the Geneva–Copenhagen Survey (Nordström et al. 2004; Holmberg, Nordström & Andersen 2007, 2009).

For calculating the effective temperature, we have used the bolometric flux determined from spectrophotometry by Boyajian et al. (2013) (see Table 1). In addition to the formal errors quoted by Boyajian et al. (2013), we include an additional 1 per cent uncertainty accounting for systematics present in the absolute flux calibration of photometric data (see discussion in Bessell & Murphy 2012). Our measured temperature for θ Cyg (6749 $\pm$ 44 K) is in excellent agreement with the values determined by Erspamer & North (2003) from spectroscopy (6745 $\pm$ 150 K) and Ligi et al. (2012) from interferometry (6767 $\pm$ 87 K).

Fig. 2 shows a histogram of the MIRC closure phase measurements. All values are consistent with zero, indicating that the source has a point-symmetric intensity distribution. Ligi et al. (2012) reported that the scatter in their measurements of θ Cyg with the VEGA beam combiner was higher than expected, leaving open the possibility of stellar variations or a close companion. As they noted, *Kepler* observations would have detected any large stellar pulsations, and so this explanation for their result is unsatisfactory.

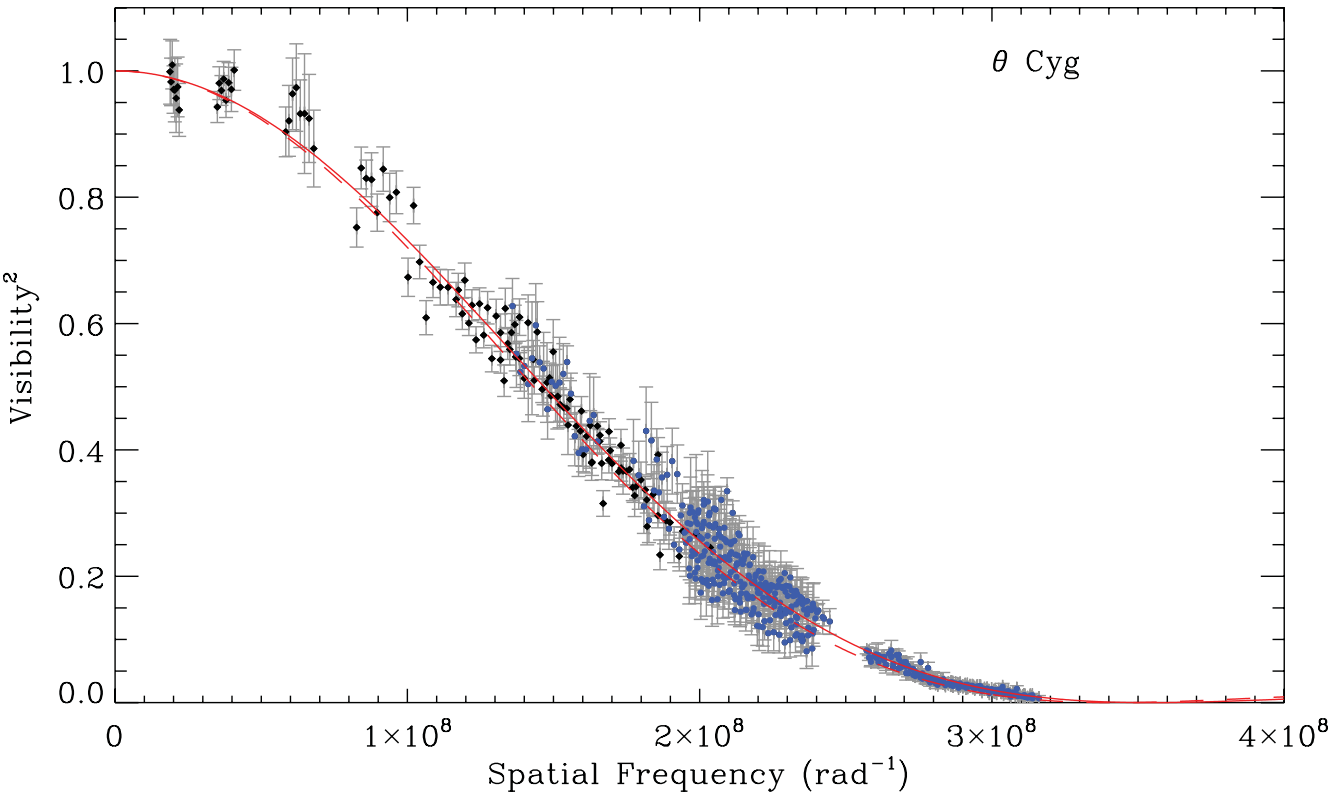

Figure 1. Squared visibility versus spatial frequency for θ Cyg for PAVO (blue circles) and MIRC (black diamonds) data. The red lines show the fitted limb-darkened model to the combined data. The solid line is for $\mu = 0.47 \pm 0.04$ (PAVO) while the dashed line is for $\mu = 0.21 \pm 0.03$ (MIRC).

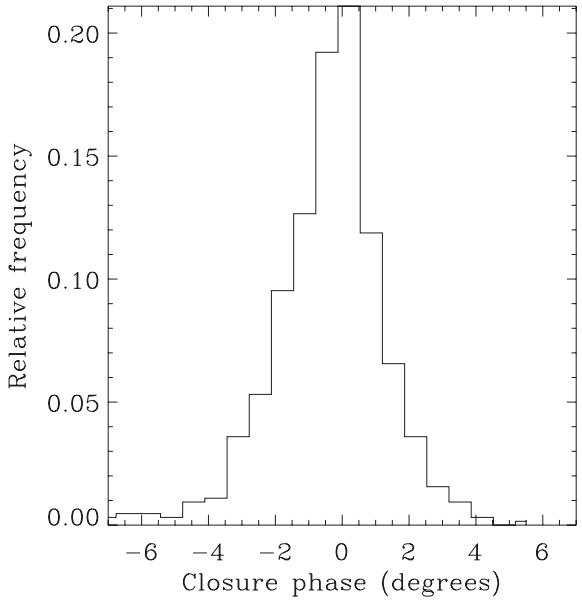

Figure 2. Histogram of MIRC closure phase measurements for θ Cyg.

Our MIRC closure phase measurements also appear to rule out a new close companion. Following the method used by Kraus et al. (2008), we estimated the detection threshold for a close companion as a function of separation. Briefly, this method involves Monte Carlo simulations of data sets with the same (u, v)-sampling and error properties of our MIRC observations and finding the best-fitting contrast ratio within a large grid of positions and separations. The 99.9 per cent upper limit to companion brightness within a series of annuli was determined as the contrast ratio for which 99.9 per cent of simulations had no companion brighter than this limit anywhere within the annulus. We find that a potential close companion with a separation between 10 and 20 mas (∼0.2–0.4 au) must be at least 4.68 mag fainter in H band than θ Cyg to escape detection in our observations. For separations between 20 and 40 mas (∼0.4–0.7 au), the companion must be at least 3.44 mag fainter.

4.3 16 Cyg A and B

Fig. 3 shows the calibrated squared-visibility PAVO and Classic measurements as a function of spatial frequency for 16 Cyg A and B. As for θ Cyg, we provide the fitted uniform-disc and limb-darkened diameters, along with derived properties in Table 4. Inclusion of the Classic data in the fit does not significantly change the measured diameters.

The diameters as measured individually with PAVO and Classic agree within the uncertainties. Our 16 Cyg B measurement is 1.1σ larger than the diameter measured by Baines et al. (2008, $\theta_{\rm LD}$ = 0.426 ± 0.056 mas), although their estimate from spectral energy distribution fitting ($\theta_{\rm LD} = 0.494 \pm 0.019$ mas) is in excellent agreement with our final value.

The larger uncertainties in our Classic diameters compared to the values reported by Boyajian et al. (2013) arise largely from the inclusion of additional uncertainty in the linear limb-darkening coefficient. It is also worth noting that whereas we determined the limb-darkening coefficient from the model grid of Claret & Bloemen (2011), Boyajian et al. (2013) used the values from Claret (2000), leading to slightly different values being used.

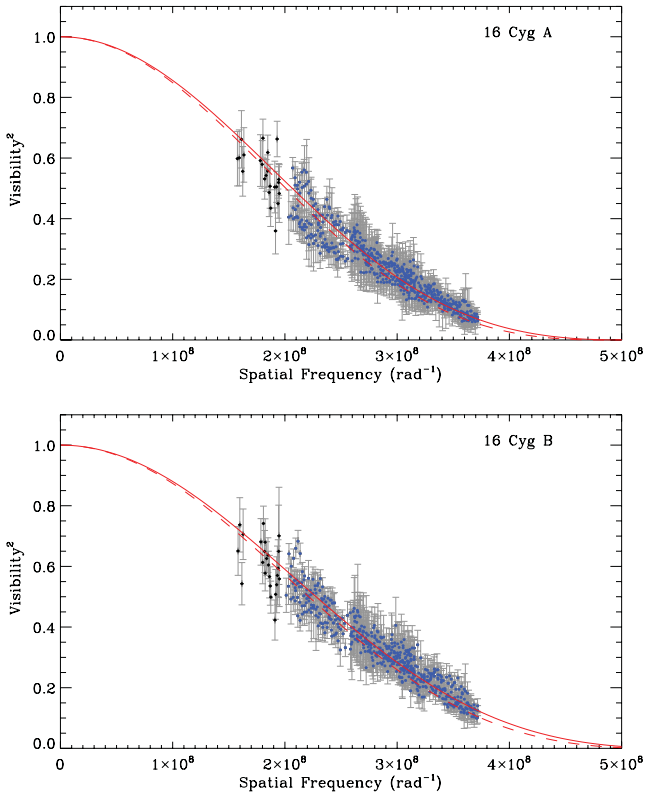

Figure 3. Squared visibility versus spatial frequency for 16 Cyg A (top) and B (bottom) for PAVO (blue circles) and Classic (black diamonds) data. The red lines show the fitted limb-darkened model to the combined data. The solid lines use the limb-darkening coefficients in R band (PAVO) while the dashed line is for H band (Classic). Note that the error bars for each star have been scaled so that the reduced χ^2 equals unity.

We are able to compare our measured radii and masses with those obtained by preliminary asteroseismic modelling by Metcalfe et al. (2012). Several different approaches were taken to model the pair, using measured oscillation frequencies and spectroscopic values as constraints. Methods varied with different stellar evolutionary and pulsation codes, nuclear reaction rates, opacities, and treatments of diffusion and convection used.

As mentioned in Section 2.2, the best-fitting model of each method fell into one of two families. A low-radius, low-mass family favoured R = 1.24 $R_\odot$, M = 1.10 $M_\odot$ for 16 Cyg A and R = 1.12 $R_\odot$, M = 1.05 $M_\odot$ for 16 Cyg B. The high-radius, high-mass family favoured R = 1.26 $R_\odot$, M = 1.14 $M_\odot$ and R = 1.14 $R_\odot$, M = 1.09 $M_\odot$, respectively.

Comparison with our results in Table 4 shows a preference for the low-radius, low-mass family, although the high-radius, high-mass family cannot be completely discounted, particularly for 16 Cyg B. This brief comparison suggests that, in conjunction with more *Kepler* data that are becoming available, our interferometric results will help to significantly constrain stellar models.

When calculating the effective temperature, we have again used the bolometric flux determined by Boyajian et al. (2013), once again adopting an additional 1 per cent uncertainty to account for systematics in the absolute flux calibration. As for θ Cyg, our measured temperatures (5839 ± 42 and 5809 ± 39 K for 16 Cyg A and B, respectively) agree well with the spectroscopically determined values (5825 ± 50 and 5750 ± 50 K; Ramírez et al. 2009).

4.4 Comparison with asteroseismic scaling relations

In addition to the scaling relation for the large frequency separation, $\Delta\nu$, given in equation (5), there is also a widely used scaling relation for the frequency of maximum power, $\nu_{\rm max}$ (Brown et al. 1991; Kjeldsen & Bedding 1995):

$$\frac{\nu_{\rm max}}{\nu_{\rm max,\odot}} = \left(\frac{M}{\rm M_\odot}\right)\left(\frac{R}{\rm R_\odot}\right)^{-2}\left(\frac{T_{\rm eff}}{\rm T_{eff,\odot}}\right)^{-1/2}. \quad (6)$$

Equations (5) and (6) may be simultaneously solved for mass and radius:

$$\frac{M}{\rm M_\odot} = \left(\frac{\nu_{\rm max}}{\nu_{\rm max,\odot}}\right)^{3}\left(\frac{\Delta\nu}{\Delta\nu_\odot}\right)^{-4}\left(\frac{T_{\rm eff}}{\rm T_{eff,\odot}}\right)^{3/2} \quad (7)$$

and

$$\frac{R}{\rm R_\odot} = \left(\frac{\nu_{\rm max}}{\nu_{\rm max,\odot}}\right)\left(\frac{\Delta\nu}{\Delta\nu_\odot}\right)^{-2}\left(\frac{T_{\rm eff}}{\rm T_{eff,\odot}}\right)^{1/2}. \quad (8)$$

Provided the effective temperature is known, the stellar mass and radius may be estimated directly from the asteroseismic parameters $\Delta\nu$ and $\nu_{\rm max}$. This is sometimes referred to as the 'direct method' (Kallinger et al. 2010a; Chaplin et al. 2011; Silva Aguirre et al. 2011) in contrast to determining mass, radius and other parameters via stellar modelling (Stello et al. 2009b; Basu, Chaplin & Elsworth 2010; Kallinger et al. 2010b; Gai et al. 2011).

The scaling relation for $\Delta\nu$, which we have used to derive the masses in Table 4, is better understood theoretically with tests of its validity in models finding the relation holds to within 5 per cent (Stello et al. 2009a; White et al. 2011). The $\nu_{\rm max}$ scaling relation relies on the argument that $\nu_{\rm max}$ should scale with the acoustic cut-off frequency (Brown et al. 1991), although the underlying physical reason for this relationship has not been clear. Only recently has the theoretical framework behind this result begun to be developed (Belkacem et al. 2011). Understanding the validity of these scaling relations has become particularly important as they are now commonly used to determine radii for a large number of faint *Kepler* stars, including some stars with detected exoplanet candidates (see e.g. Borucki et al. 2012; Huber et al. 2013). We are able to test the validity of the asteroseismic scaling relations by comparing our interferometric radii with independently determined asteroseismic radii calculated using equation (8). To ensure that the asteroseismic radii are truly independent of our interferometric radii, in this calculation we use the spectroscopic effective temperatures given in Table 1.

We have determined the global asteroseismic properties, $\Delta\nu$ and $\nu_{\rm max}$, of 16 Cyg A and B using the automated analysis pipeline by Huber et al. (2009), which has been shown to agree well with other methods (Hekker et al. 2011; Verner et al. 2011). These values are given in Table 5, along with the radii derived from the scaling relations, equations (5) and (6). We use solar values of $\Delta\nu_\odot = 135.1$ μHz and $\nu_{\rm max,\odot} = 3090$ μHz.

We do not consider θ Cyg here because the width of the oscillation envelope is very broad, which makes $\nu_{\rm max}$ ambiguous. This, along with large mode linewidths (Chaplin et al. 2009; Baudin et al. 2011; Appourchaux et al. 2012; Corsaro et al. 2012), appears to be a feature of oscillations in F stars. Observations of the F subgiant Procyon showed a similarly broad envelope (Arentoft et al. 2008).

Table 5. Asteroseismic properties and radii of 16 Cyg A and B.

	16 Cyg A	16 Cyg B
$\Delta\nu$ (μHz)	103.5 ± 0.1	117.0 ± 0.1
$\nu_{\rm max}$ (μHz)	2201 ± 20	2552 ± 20
R ($\rm R_\odot$)	1.218 ± 0.012	1.098 ± 0.010

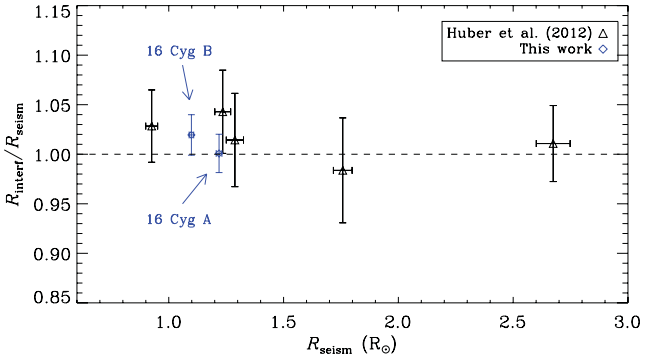

Figure 4. Comparison of stellar radii measured using interferometry and calculated using asteroseismic scaling relations. The black triangles show stars measured by Huber et al. (2012b), while the blue diamonds show 16 Cyg A and B.

Fig. 4 shows the remarkable agreement between the interferometric and asteroseismic radii. In addition to 16 Cyg A and B, we also include five stars for which Huber et al. (2012b) determined interferometric and asteroseismic radii using the same method (see their fig. 7). The agreement for 16 Cyg A and B is within 1σ and at an ∼2 per cent level, which makes this the most precise independent empirical test of asteroseismic scaling relations yet. However, further studies are still needed, particularly of stars that are significantly different from the Sun, to robustly test the validity of the scaling relations.

5 CONCLUSIONS

We have used long-baseline interferometry to measure angular diameters for θ Cyg and 16 Cyg A and B. All three stars have been observed by the *Kepler Mission* and exhibit solar-like oscillations, allowing for detailed study of their internal structure.

For θ Cyg, we find a limb-darkened angular diameter of $\theta_{\rm LD} = 0.753 \pm 0.009$ mas, which, combined with the Hipparcos parallax, gives a linear radius of $R = 1.48 \pm 0.02$ $\rm R_\odot$. When determining the mass (1.37 ± 0.04 $\rm M_\odot$) from the interferometric radius and large frequency separation, $\Delta\nu$, we find that it is necessary to use the revised scaling relation for $\Delta\nu$ suggested by White et al. (2011). This revision takes into account a deviation from the standard scaling relation in stars of higher temperature, without which the determined mass would be significantly lower (1.27 $\rm M_\odot$) than expected from fitting to isochrones.

Closure phase measurements of θ Cyg reveal the star to be point symmetric, consistent with being a single star. This rules out the possibility of all but a very low luminosity close companion, which had previously been suggested.

For 16 Cyg A and B, we have found limb-darkened angular diameters of $\theta_{\rm LD} = 0.539 \pm 0.007$ and $\theta_{\rm LD} = 0.490 \pm 0.006$, and linear radii of $R = 1.22 \pm 0.02$ and 1.12 ± 0.02 $\rm R_\odot$, respectively. Comparing these radii with those derived from the asteroseismic scaling relations shows good agreement at an ∼2 per cent level.

Our measurements of near-model-independent masses, radii and effective temperatures will provide strong constraints when modelling these stars.

ACKNOWLEDGEMENTS

The CHARA Array is funded by the National Science Foundation through NSF grant AST-0606958, by Georgia State University

through the College of Arts and Sciences and by the W.M. Keck Foundation. We acknowledge the support of the Australian Research Council. Funding for the Stellar Astrophysics Centre is provided by The Danish National Research Foundation. We also acknowledge the Kepler Science Team and all those who have contributed to the *Kepler Mission*. Funding for the *Kepler Mission* is provided by NASA's Science Mission Directorate. TRW is supported by an Australian Postgraduate Award, a University of Sydney Merit Award, an Australian Astronomical Observatory PhD Scholarship and a Denison Merit Award. DH is supported by an appointment to the NASA Postdoctoral Program at Ames Research Center, administered by Oak Ridge Associated Universities through a contract with NASA.

REFERENCES

Aerts C., Christensen-Dalsgaard J., Kurtz D. W., 2010, Asteroseismology. Springer, Dordrect
Appourchaux T. et al., 2012, A&A, 537, A134
Arentoft T. et al., 2008, ApJ, 687, 1180
Baines E. K., McAlister H. A., ten Brummelaar T. A., Turner N. H., Sturmann J., Sturmann L., Goldfinger P. J., Ridgway S. T., 2008, ApJ, 680, 728
Baines E. K., McAlister H. A., ten Brummelaar T. A., Sturmann J., Sturmann L., Turner N. H., Ridgway S. T., 2009, ApJ, 701, 154
Barnes T. G., Evans D. S., Moffett T. J., 1978, MNRAS, 183, 285
Basu S., Chaplin W. J., Elsworth Y., 2010, ApJ, 710, 1596
Baudin F. et al., 2011, A&A, 529, A84
Bazot M. et al., 2011, A&A, 526, L4
Belkacem K., 2012, in Boissier S., de Laverny P., Nardetto N., Samadi R., Valls-Gabaud D., Wozniak H., eds, SF2A-2012: Proc Annual Meeting French Soc. Astron. Astrophys. SF2A, Paris, p. 173
Belkacem K., Goupil M. J., Dupret M. A., Samadi R., Baudin F., Noels A., Mosser B., 2011, A&A, 530, A142
Bessell M. S., 2000, PASP, 112, 961
Bessell M., Murphy S., 2012, PASP, 124, 140
Bigot L., Kervella P., Thévenin F., Ségransan D., 2006, A&A, 446, 635
Bonneau D. et al., 2006, A&A, 456, 789
Bonneau D., Delfosse X., Mourard D., Lafrasse S., Mella G., Cetre S., Clausse J.-M., Zins G., 2011, A&A, 535, A53
Borucki W. J. et al., 2012, ApJ, 745, 120
Boyajian T. S. et al., 2009, ApJ, 691, 1243
Boyajian T. S. et al., 2012a, ApJ, 746, 101
Boyajian T. S. et al., 2012b, ApJ, 757, 112
Boyajian T. S. et al., 2013, ApJ, in press
Brown T. M., Gilliland R. L., 1994, ARA&A, 32, 37
Brown T. M., Gilliland R. L., Noyes R. W., Ramsey L. W., 1991, ApJ, 368, 599
Bruntt H. et al., 2010, MNRAS, 405, 1907
Cardelli J. A., Clayton G. C., Mathis J. S., 1989, ApJ, 345, 245
Casagrande L., Schönrich R., Asplund M., Cassisi S., Ramírez I., Meléndez J., Bensby T., Feltzing S., 2011, A&A, 530, A138
Chaplin W. J., Houdek G., Karoff C., Elsworth Y., New R., 2009, A&A, 500, L21
Chaplin W. J. et al., 2011, Sci, 332, 213
Che X., Monnier J. D., Webster S., 2010, in Danchi W. C., Delplancke F., Rajagopal J. K., eds, Proc. SPIE Vol. 7734, Optical and Infrared Interferometry II. SPIE, Bellingham, p. 77342V
Che X., Monnier J. D., Kraus S., Baron F., Pedretti E., Thureau N., Webster S., 2012, in Delplancke F., Rajagopal J. K., Malbet F., eds, SPIE Vol. 8445, Optical and Infrared Interferometry III. SPIE, Bellingham, p. 84550Z
Chiavassa A., Collet R., Casagrande L., Asplund M., 2010, A&A, 524, A93
Chiavassa A., Bigot L., Kervella P., Matter A., Lopez B., Collet R., Magic Z., Asplund M., 2012, A&A, 540, A5
Christensen-Dalsgaard J., 2004, Sol. Phys., 220, 137
Claret A., 2000, A&A, 363, 1081
Claret A., Bloemen S., 2011, A&A, 529, A75
Cochran W. D., Hatzes A. P., Butler R. P., Marcy G. W., 1997, ApJ, 483, 457
Code A. D., Bless R. C., Davis J., Brown R. H., 1976, ApJ, 203, 417
Corsaro E. et al., 2012, ApJ, 757, 190
Creevey O. L. et al., 2012, A&A, 545, A17
Cunha M. S. et al., 2007, A&AR, 14, 217
Deheuvels S., Michel E., 2011, A&A, 535, A91
Demarque P., Guenther D. B., van Altena W. F., 1986, ApJ, 300, 773
Derekas A. et al., 2011, Sci, 332, 216
Desort M. et al., 2009, A&A, 506, 1469
Drimmel R., Cabrera-Lavers A., López-Corredoira M., 2003, A&A, 409, 205
Erspamer D., North P., 2003, A&A, 398, 1121
Gai N., Basu S., Chaplin W. J., Elsworth Y., 2011, ApJ, 730, 63
Gilliland R. L. et al., 2010, PASP, 122, 131
Guzik J. A. et al., 2011, preprint (arXiv:1110.2120)
Hanbury Brown R., Davis J., Lake R. J. W., Thompson R. J., 1974, MNRAS, 167, 475
Hauser H. M., Marcy G. W., 1999, PASP, 111, 321
Hekker S. et al., 2011, A&A, 525, A131
Holmberg J., Nordström B., Andersen J., 2007, A&A, 475, 519
Holmberg J., Nordström B., Andersen J., 2009, A&A, 501, 941
Huber D., Stello D., Bedding T. R., Chaplin W. J., Arentoft T., Quirion P., Kjeldsen H., 2009, Commun. Asteroseismol., 160, 74
Huber D. et al., 2012a, MNRAS, 423, L16
Huber D. et al., 2012b, ApJ, 760, 32
Huber D. et al., 2013, ApJ, 767, 127
Ireland M. J. et al., 2008, in Schöller M., Danchi W. C., Delplancke F., eds, Proc. SPIE Vol. 7013, Optical and Infrared Interferometry. SPIE, Bellingham, p. 701324
Kallinger T. et al., 2010a, A&A, 509, A77
Kallinger T. et al., 2010b, A&A, 522, A1
Kervella P., Thévenin F., Di Folco E., Ségransan D., 2004, A&A, 426, 297
Kjeldsen H., Bedding T. R., 1995, A&A, 293, 87
Koch D. G. et al., 2010, ApJ, 713, L79
Kraus A. L., Ireland M. J., Martinache F., Lloyd J. P., 2008, ApJ, 679, 762
Ligi R. et al., 2012, A&A, 545, A5
Maestro V. et al., 2012, in Delplancke F., Rajagopal J. K., Malbet F., eds, Proc. SPIE Vol. 8445, Optical and Infrared Interferometry III. SPIE, Bellingham, p. 84550G
Mason B. D., Wycoff G. L., Hartkopf W. I., Douglass G. G., Worley C. E., 2001, AJ, 122, 3466
Metcalfe T. S. et al., 2012, ApJ, 748, L10
Michel E. et al., 2008, Sci, 322, 558
Monnier J. D., Berger J.-P., Millan-Gabet R., ten Brummelaar T. A., 2004, in Traub W. A., ed., SPIE Vol. 5491, New Frontiers in Stellar Interferometry. SPIE, Bellingham, p. 1370
Monnier J. D. et al., 2006, in Monnier J. D., Schöller M., Danchi W. C., eds, Proc. SPIE Vol. 6268, Advances in Stellar Interferometry. SPIE, Bellingham, p. 62681D
Monnier J. D. et al., 2010, in Danchi W. C., Delplancke F., Rajagopal J. R., eds, Proc. SPIE Vol. 7734, Optical and Infrared Interferometry II. SPIE, Bellingham, p. 77340G
Monteiro M. J. P. F. G., Christensen-Dalsgaard J., Thompson M. J., 1996, A&A, 307, 624
Nordström B. et al., 2004, A&A, 418, 989
North J. R. et al., 2007, MNRAS, 380, L80
O'Donnell J. E., 1994, ApJ, 422, 158
Patience J. et al., 2002, ApJ, 581, 654
Perryman M. A. C., ESA, ed., 1997, ESA SP:1200, The HIPPARCOS and TYCHO catalogues. Astrometric and photometric star catalogues derived from the ESA HIPPARCOS Space Astrometry Mission, ESA, Noordwijk
Piau L., Kervella P., Dib S., Hauschildt P., 2011, A&A, 526, A100
Ramírez I., Meléndez J., Asplund M., 2009, A&A, 508, L17
Silva Aguirre V. et al., 2011, ApJ, 740, L2
Skrutskie M. F. et al., 2006, AJ, 131, 1163

Stello D., Chaplin W. J., Basu S., Elsworth Y., Bedding T. R., 2009a, MNRAS, 400, L80
Stello D. et al., 2009b, ApJ, 700, 1589
ten Brummelaar T. A. et al., 2005, ApJ, 628, 453
Trampedach R., Stein R. F., 2011, ApJ, 731, 78
Turner N. H., ten Brummelaar T. A., McAlister H. A., Mason B. D., Hartkopf W. I., Roberts L. C., Jr, 2001, AJ, 121, 3254
Ulrich R. K., 1986, ApJ, 306, L37
van Belle G. T. et al., 2008, ApJS, 176, 276
van Leeuwen F., 2007, A&A, 474, 653
Verner G. A. et al., 2011, MNRAS, 415, 3539
White T. R., Bedding T. R., Stello D., Christensen-Dalsgaard J., Huber D., Kjeldsen H., 2011, ApJ, 743, 161

This paper has been typeset from a TEX/LATEX file prepared by the author.